J. Indian Inst. Sci. 65(A), July 1984, pp. 79-93

Mean velocity characteristics of plane diffuser flows with inlet velocity distortion

V.K. CHITHAMBARAN*
Department of Civil Engineering, Regional Engineering College, Tiruchirapalli 620 015.

P.A. ASWATHA NARAYANA AND N.V. CHANDRASEKHARA SWAMY
Department of Applied Mechanics, Indian Institute of Technology, Madras 600 026, India.

Abstract

Characteristics of flow in a straight two-dimensional diffuser with distorted inlet velocity profiles are presented. The distortion is generated by placing a symmetrical airfoil in the approaching flow at incidence to the flow direction. Static pressure recovery is less for smaller angles of incidence while it is high for larger angles when compared with uniform inlet velocity distribution. The boundary layers and wake do not exhibit equilibrium characteristics.

Key words: Two-dimensional diffuser, inlet velocity distortion, static pressure recovery, boundary layer, wake.

1. Introduction

Flow in a diffuser is in general highly complex because of the large number of parameters involved. It is very difficult to incorporate the influence of all the parameters in a theoretical model since the flow is usually turbulent. Hence, one has to rely rather heavily on experimental investigations.

It is rather rare in practice to encounter a uniform inlet flow into a diffuser. Distortion of the entry flow is more of a rule than an exception. Such a flow distortion affects the performance of a diffuser considerably. It has been shown by Waitman *et al*[1] that distortion produced by the wake of a splitter plate or cylinder improved pressure recovery in the diffuser. However, when the distortion was asymmetric, the pressure recovery performance deteriorated. The measurements of Wolf and Johnston[2] showed that the jet-type and step shear-type distortions adversely affected diffuser performance whereas wake-type entry distortions improved pressure recovery over that with undistorted entry. The better performance with wake-type inlet distortions was attributed to the rather strong mixing brought about by the interaction of the wake with the diverging wall boundary layers. These investigations show that the diffuser performance is very much dependent on the type of inlet velocity distortion induced.

* Deceased.

The objective of the present work is to investigate this type of flow in greater detail by inducing entry distortions through the use of a symmetric airfoil upstream of the diffuser. The degree of asymmetry is controlled by the angle made by the airfoil chord with the flow direction. The following cases have been investigated:

(i) Uniform core velocity
(ii) Symmetric wake-type distortion and
(iii) Non-symmetric wake-type distortion.

2. Experimental facility

The experimental facility used for this purpose was specially built and is shown schematically in fig. 1. The wind tunnel had a rectangular bell-mouth entry of size 900 × 900 mm followed by a settling length of 800 mm containing three nylon screens for damping the disturbances and spatial irregularities of the flow. This was followed by a two-dimensional contraction of ratio 6 to 1, which reduced the section to 150 × 600 mm. A constant rectangular channel section of the same dimension and length of 494 mm connected the contraction to a straight walled test diffuser which had a length of 1195 mm. The area ratio of the diffuser was 2 to 1 and the entry aspect ratio was 4. This diffuser was designed based on

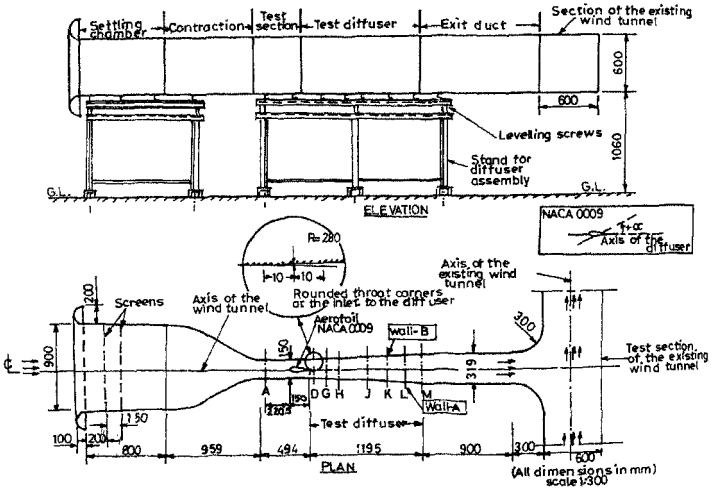

FIG. 1. Sketch of the wind tunnel.

the chart of Reneau *et al*[3]. The diffuser was led at right angles through a bell-mouth exit into the test-section of another open-circuit wind tunnel, which was powered by a 27 KW DC motor with a fan.

Distortion in the inlet velocity profile was produced by placing a NACA 0009 airfoil of chord-length 150 mm ahead of the diffuser spanning the 600 mm height of the test section. The airfoil was placed centrally such that its trailing edge was at the inlet to the diffuser. Non-symmetric distortion was generated by placing the airfoil at an incidence to the flow. The incidence angle of the airfoil was limited to 10°, well below the stall angle of the airfoil.

The wind tunnel was calibrated before use. At the inlet to the diffuser, it was observed that mean velocity profiles across the width of the channel at several elevations varied within 0.5% of that in the axial plane, thus indicating two-dimensional flow conditions. Since the diffuser was made of plexiglass, flow visualisation with woollen tufts was possible. This indicated no sign of flow separation anywhere inside the diffuser or over a length of about 600 mm downstream of the diffuser exit, for the range of angles of incidence of the airfoil for which the investigations were conducted.

Measurements of wall static pressure were done with 0.5 mm diameter tappings and were subjected to wall displacement correction as described by Pierce and Zimmermann[4]. Total and static pressures in the flow were measured by standard calibrated probes. The static pressure probe had an outer diameter of 1 mm with four peripheral holes of 0.3 mm diameter. The total pressure probe was also of 1 mm in diameter with a 0.6 mm diameter hole at the mouth. Pressures were measured with standard Betz, Prandtl and inclined tube manometers. Turbulence in the flow introduces errors when measurements are made with static and total pressure probes. Calculations based on Irwin's equation[5] showed that the maximum error in the mean velocity was of the order of 0.81% at a station near the inlet and 0.97% at a station near the exit of the diffuser for $\alpha = 0°$. For $\alpha = 4°$, the maximum error was of the order of 1.2% and 1.75% respectively near the inlet and the exit of the diffuser.

The measurement stations are indicated in fig. 2. The stations designated as D to M were along the axis of the diffuser. The location of these stations from the diffuser inlet is indicated in Table I.

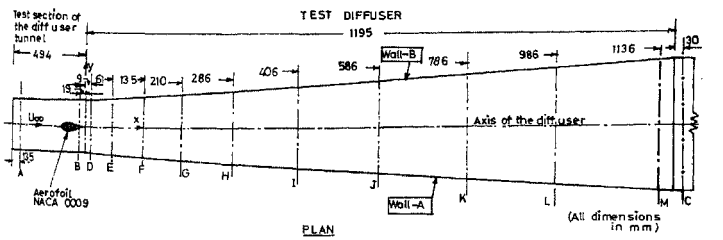

FIG. 2. Location of the measurement stations.

Table I

Location of measurement stations

Measurement Stations	D	E	F	G	H	I	J	K	L	M
Distance X in mm	9	61	135	210.5	286	406	586	786	986	1136
X/c	0.060	0.406	0.900	1.403	1.906	2.706	3.906	5.24	6.57	7.57
X/L	0.0075	0.051	0.113	0.176	0.239	0.340	0.491	0.659	0.826	0.952

3. Results and discussion

3.1. Diffuser performance

The variation of the normalised static pressure along the diffuser walls is shown in fig. 3. The pressure distribution near the diffuser inlet is considerably altered by the presence of the airfoil upstream, but settles down quickly within about two chord-lengths downstream of the airfoil trailing edge, even for $\alpha = 10°$. Measurements, not indicated in fig. 3, showed that the wall static pressure distribution along the wall-A for $\alpha = 4°$ was almost the same as that along the wall-B for $\alpha = -4°$.

The average wall static pressure at station-B, 19 mm upstream of the diffuser inlet, was measured in the absence of the airfoil from 10 wall static pressure taps distributed around the periphery. Similarly, the average pressure at station-C, 30 mm downstream of the diffuser exit, was obtained from eight static pressure taps distributed around the periphery. The average static pressure recovery coefficient was then calculated from the formula

$$\bar{C}_p = \frac{\bar{P}_C - \bar{P}_B}{\bar{q}_B} \tag{1}$$

The value was found to be 0.645 which compares favourably with a value of 0.655 which is obtained by interpolation from the chart of Reneau *et al*[3] for an inlet blockage of 0.024.

When the airfoil was introduced at the diffuser inlet, station B was no longer accessible for the traverse. Hence the average static pressure obtained from the measured wall static pressure distribution on walls-A and -B and the dynamic pressure based on the average velocity at station D, which is 9 mm downstream of the inlet, were made use of in calculating the static pressure recovery coefficient along the diffuser for all the cases investigated. This gave a $\bar{C}_P$ value of 0.747 for the case without the airfoil. With the airfoil, the $\bar{C}_P$ values were 0.696 at $\alpha = 0°$, 0.632 at $\alpha = 4°$, 0.831 at $\alpha = 7°$ and 0.814 at $\alpha = 10°$. The presence of the airfoil noticeably reduces the pressure recovery for low values of α. But at $\alpha = 7°$, the pressure recovery rises to 0.831 and drops to 0.814 at $\alpha = 10°$. The large $\bar{C}_P$ for $\alpha = 7°$ is

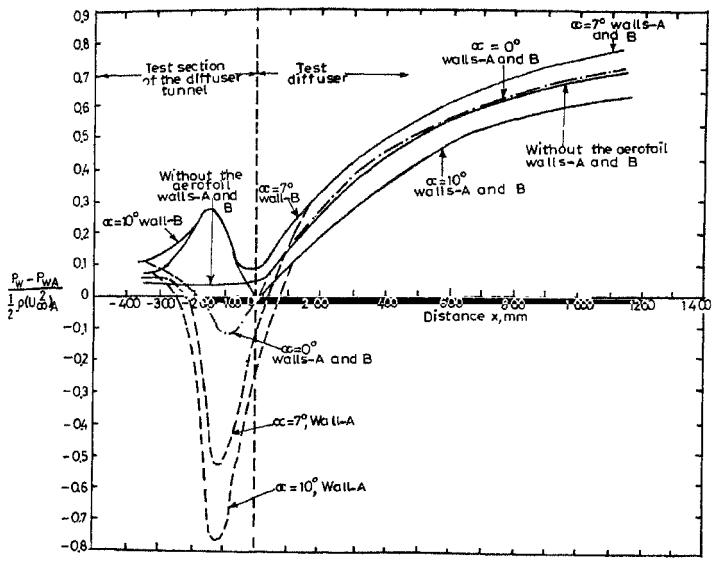

FIG. 3. Wall static pressure distribution.

probably due to strong interaction between the wall shear layer and the airfoil wake, promoting bulk mixing. This condition corresponds to a minimum increase in displacement thickness of the wall boundary layer as also noted by Schubauer and Spangenberg[6]. This type of behaviour has also been observed by Waitman *et al*[1] and Wolf and Johnston[2]. It was also seen that about 80% of the pressure recovery was attained within the initial 50% of the diffuser length.

The blockage factor B was calculated at the diffuser inlet based on the velocity profile data. The value of B increased progressively from 2.4% for the case without airfoil to 5.6% for $\alpha=0°$, to 6.6% of $\alpha=4°$, to 8.3% for $\alpha=7°$ and to 12.2% for $\alpha=10°$. This shows that irrespective of pressure recovery, increasing or decreasing, the blockage factor continuously increases, which is quite contrary to the conclusion of Sovran and Klomp[7] that pressure decreases continuously with increasing blockage. But in their case, inlet blockage was of the boundary layer type whereas in the present case the blockage is mainly due to the distortion of core velocity at inlet. Apparently, there is no simple and monotonic relationship between pressure recovery and blockage factor for the present case.

To consider this point in greater detail, the total blockage factor along the diffuser without airfoil and with airfoil for $\alpha=0°$ and $10°$ is shown in fig. 4. The total blockage here is the sum of the boundary layer blockage at the walls and the wake blockage at the core. It can be seen from this figure that the blockage increases more or less monotonically along the diffuser in the absence of the airfoil but shows a waviness when the airfoil is present. To analyse this further, the blockage due to the wake and that due to the boundary layer separately for $\alpha=0°$ and $10°$ are shown in fig. 5. The blockage due to the wall boundary layer exhibits a smooth increase along the diffuser length but the one due to the wake shows a wavy behaviour. The wake blockage not only does not increase monotonically but also oscillates about a mean position slightly smaller than the initial value. This is more pronounced for the case of larger incidence. When the airfoil is at incidence, the wake and its growth rate exhibited asymmetric characteristics about the diffuser axis. Spectral measurements[8] made in this region exhibited a predominant frequency suggesting the possible existence of a vortex shedding.

3.2 Wall boundary layer characteristics

The development of boundary layer velocity profiles on both walls-A and -B was examined for all the cases.

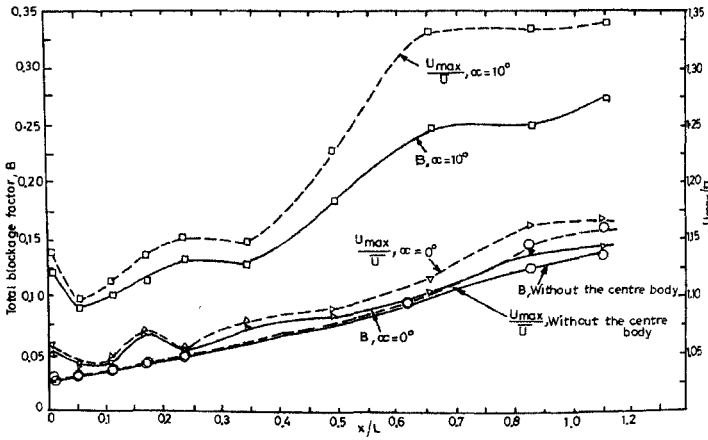

FIG. 4. Development of total blockage factor B along the diffuser.

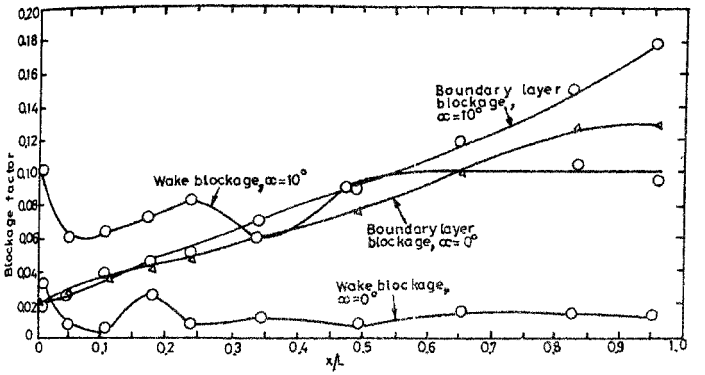

FIG. 5. Blockage due to boundary layer and blockage due to wake.

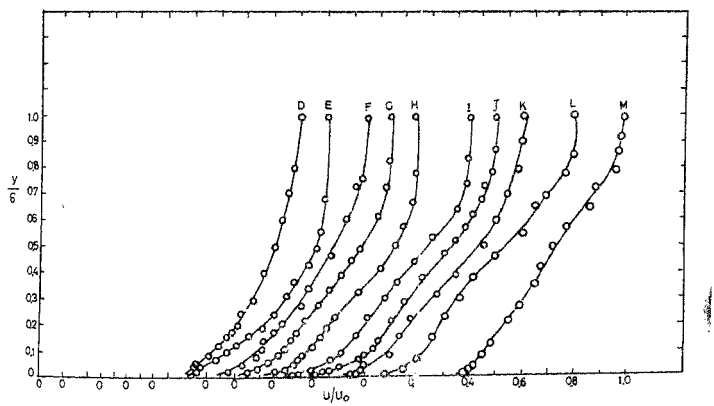

FIG. 6. Mean velocity profile in the boundary layer on wall-B, $\alpha = 0°$.

Wall shear stress was calculated by the method of Clauser[9] using a computer programme. The values so obtained were checked against those from the conventional graphical method

for $\alpha = 10°$ and the agreement was found to be satisfactory. The values are presented for wall-B in fig. 7. These values also compare favourably with the values obtained from the use of Ludwig-Tillmann formula[10] except near the inlet to the diffuser, where the latter gave values lower by about 12%. For $\alpha = 10°$, the skin-friction coefficient decreased from 0.0053 at station D to 0.0014 at station M on wall-B, whereas on wall-A the corresponding values were respectively 0.0035 and 0.00061.

With the estimated values of skin-friction, the log-law was satisfied up to $y^+ = 250$. For $\alpha = 10°$, the profiles on wall-B had a larger log-law region than those on wall-A, which is obviously due to the larger c_f values on wall-B. However, at low values of c_f, the flow is pretty close to separation and estimation of skin-friction coefficient from Clauser's method becomes unreliable. This is true not only for the present data but also for those of Spangenberg *et al*[11]

In order to test whether the wall layers exhibited any equilibrium characteristics, the equilibrium parameter given by

$$G = \int_0^\infty \left(\frac{U_0 - U}{u_\tau}\right)^2 \mathrm{d}y \Big/ \int_0^\infty \left(\frac{U_0 - U}{u_\tau}\right) \mathrm{d}y \tag{2}$$

was calculated. The value of G was found to vary considerably along the diffuser. Figure 8 shows the relationship between G and the pressure gradient parameter $\frac{\delta^*}{\tau_w}\frac{\mathrm{d}p}{\mathrm{d}x}$ given by Nash[12] *viz.*,

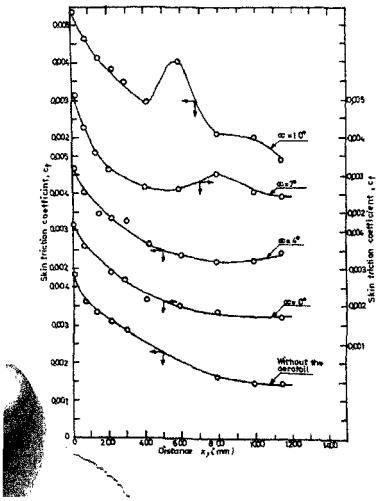

FIG. 7. Variation of skin-friction coefficient (c_f) on wall-B

$$\frac{\delta^*}{\tau_w}\frac{dp}{dx} = \left(\frac{G+1.7}{6.1}\right)^2 - 1.81 \tag{3}$$

compared with the present data showing that the boundary layers were not of equilibrium type. The correlation of Nash is well borne out by the present experiments.

Integral parameters for the wall layers, *viz.*, the displacement thickness, the momentum thickness and the shape factor calculated by integrating the measured velocity profile, agreed quite well with those calculated from the law of the wake due to Coles [13]. For $\alpha = 4°$, 7° and 10°, δ^* on wall-A was found to be generally larger than that on wall-B. Schubauer and Spangenberg [6] have shown that turbulent mixing has the possible effect of decreasing the rate of growth of the displacement thickness in a boundary layer. Hence it follows that the region in the diffuser where the increase in displacement thickness is minimum corresponds to the region having maximum mixing. Figure 9 shows that when $\alpha = 7°$, maximum mixing can be expected in the boundary layer on wall-B while when $\alpha = 10°$, the amount of mixing can get reduced. Bulk mixing is also associated with a corresponding increase in static pressure recovery [2]. It has been remarked earlier in section 3.1 that static pressure recovery is the highest for $\alpha = 7°$.

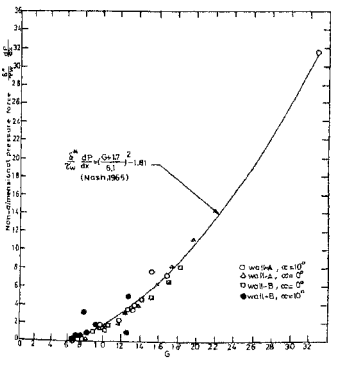

FIG. 8. Relation between Clauser's G and $\frac{\delta^*}{\tau_w}\frac{dp}{dx}$.

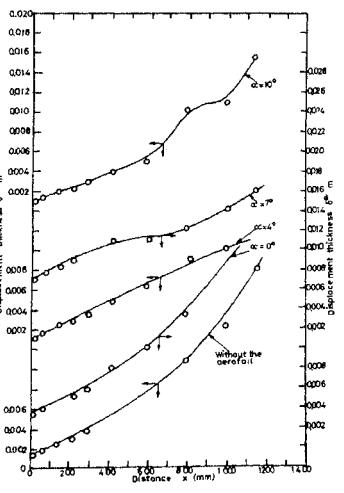

FIG. 9. Displacement thickness for the boundary layer on wall-B.

The shape factor H at station M on wall-A varies from 1.82 at $\alpha = 0°$ to 2.35 at $\alpha = 10°$. This is mainly due to the distortion in the inlet velocity profile. Tuft studies showed no indication anywhere of flow separation. It is, of course, known that in diffuser flows separation may occur over a wide range of values of H, *viz.*, between 1.8 and 3.0[14].

3.3 Behaviour of the wake

The wake axis corresponds to the position of maximum defect velocity W_0 in the wake. The wake half-width is represented by the distance from the axis at which the defect velocity reaches half its maximum value and is usually taken as the length scale for the wake. Figure 10 shows the spread of the wake described by the change in wake axis relative to diffuser axis and increase in half-width along the diffuser, both for $\alpha = 7°$ and $\alpha = 10°$. The growth of the *half-width can be well represented by* a straight line, though it differs from the $x^{1/2}$-relation valid for a two-dimensional free symmetric wake. A similar behaviour was noticed for other cases also.

The mean velocity distribution in the wake when analysed indicated asymmetry. Asymmetry increased with increase in angle of attack and was marked in the regions near the trailing edge. The wake decayed very slowly towards the exit of the diffuser. To examine whether the defect profiles exhibited any similarity, fig. 11 has been plotted for $\alpha = 7°$ and 10°. The deflect velocity W is normalised with the maximum defect velocity W_0 and the distance y from the wake axis is normalised with respect to the wake half-width. The figure shows similarity in defect velocity distribution developing within two chord-lengths downstream of

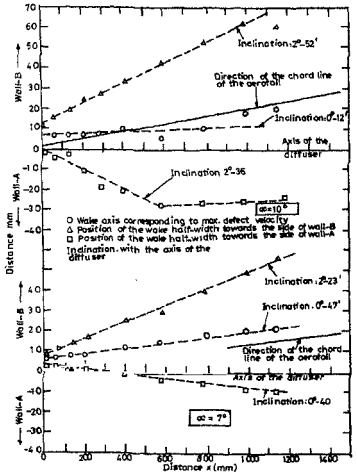

FIG. 10. Spread of the half-width of the wake and the wake axis, $\alpha = 7°$ and $\alpha = 10°$.

the airfoil trailing edge. The measured values at station J appear to be out of line at $\alpha = 7°$. This might be due to a possible error in measurement, since no such discrepancy is seen at $\alpha = 10°$. The defect velocity distribution can be empirically fitted by the equation

$$W/W_0 = \exp(-\eta^2 \ln 2), \tag{4}$$

Since the half-width towards wall-A and -B are different, the corresponding values of the half-width have been used in comparing the above empirical expression with the experimental data for $\alpha = 7°$ and $\alpha = 10°$ in fig. 11. However, this self-similarity appears to be only apparent since the agreement is not very good when considering the momentum integral for the wake. A consequence of the validity of velocity profile similarity even when the flow is not in equilibrium is that the momentum integral M for the wake should be constant. Figure 12 shows the momentum integral M normalised with the value M_1 at station D for all the

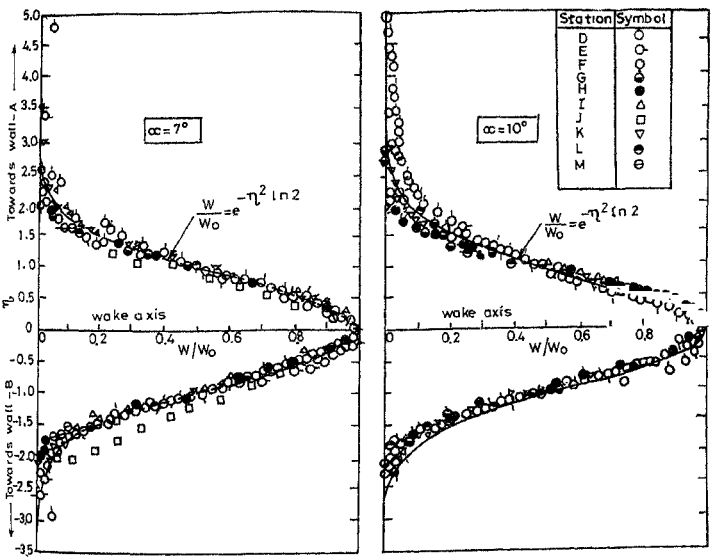

FIG. 11. Defect velocity profile for the wake, $\alpha = 7°$ and $\alpha = 10°$.

cases considered. Even accounting for possible errors in numerical integration, the variation appears too large for self-similarity to be real. This suggests that the normalised velocity profiles as in fig. 11 conceal certain characteristics of the flow and the inferences that can be drawn from such a plot may be, to some extent, misleading. Calculations also showed that for $\alpha = 0°$ and 4°, the momentum thickness of the wake increases slowly, but the rate becomes faster for $\alpha = 7°$ and 10°. The shape factor calculated for the wake varies between 1.05 and 1.35, increasing with distortion. A shape factor equation has been proposed by Spence[15] for free wakes behind airfoils in the form

$$1 - 1/H_W = (1 - 1/H_{W1})\ (40\ \frac{x}{c} + 1)^{-1/2}. \tag{5}$$

Even though this expression serves quite well for a free wake as found by Raj and Lakshminarayana[16], it does not fit the present measurements in a confined wake. The discrepancy has been found to be about 4% for $\alpha = 0°$, 6% for $\alpha = 4°$ and about 25% for $\alpha = 10°$, the experimental values being on the higher side.

The decay in the maximum velocity defect in the wake is shown in fig. 13 for $\alpha = 7°$. The velocity defect decreases by about 90% in a relatively short distance of two chord lengths.

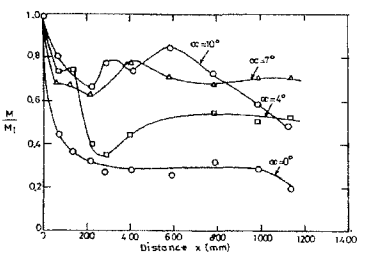

FIG. 12. Momentum integral for the wake.

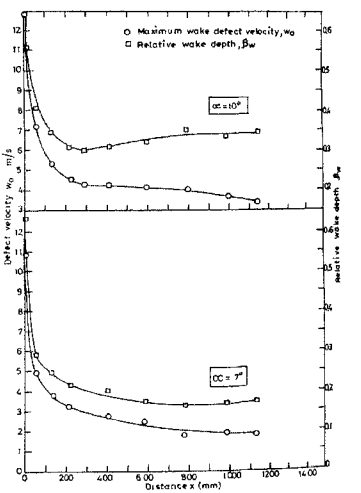

FIG. 13. Maximum wake defect, $\alpha = 7°$ and $\alpha = 10°$

The relative 'wake depth' is also shown in the same figure, which has more or less the same behaviour as the normalised velocity defect. This variation is representative of all the cases investigated.

4. Concluding remarks

Distortion of inlet velocity profile in a two-dimensional diffuser has considerable influence on its performance. The mean wall static pressure equalises rapidly within a distance of about two-chord lengths downstream of the trailing edge of the airfoil. When compared with the case of no-centre body, the static pressure recovery with centre body decreases for $\alpha = 0°$ and $\alpha = 4°$ while it increases for $\alpha = 7°$. About 80 per cent of the static pressure recovery is attained within the first half of the diffuser length.

The agreement between the skin-friction coefficient c_f as obtained by Clauser's method and as obtained from using the Ludwieg-Tillmann formula is good except for the initial two-chord lengths downstream of the trailing edge of the airfoil. The wall boundary layers were far from equilibrium.

The mean velocity distribution in the wake indicated asymmetry but when analysed in the defect form exhibited apparent similarity after two chord-lengths downstream from the trailing edge of the airfoil, even though the momentum integral did not remain constant in the streamwise direction. The momentum thickness of the wake increases gradually in the streamwise direction for $\alpha = 0°$ and $\alpha = 4°$ whereas the increase is more rapid for $\alpha = 7°$ and $\alpha = 10°$. The wake decay is rapid over the initial two-chord lengths. The growth of half-width of the wake can be approximated by a straight line for all the cases except when $\alpha = 10°$.

Acknowledgement

The authors thank the referees for constructive suggestions.

Nomenclature

A	Reference station A or wall-A
B	Blockage factor ($= 1 - \bar{U}/\bar{U}_{max}$) or wall-B
b	Half-width of the wake
$\bar{C}_P$	Static pressure recovery coefficient
c	Chord length of the airfoil
c_f	Skin-friction coefficient ($= \tau_w / \frac{1}{2} \rho U_0^2$)
G	Clauser's equilibrium parameter
H	Shape factor of the boundary layer
H_w	Shape factor of the wake
H_{wt}	Shape factor of the wake at the trailing edge of the airfoil
L	Length of the side wall of the diffuser
M	Momentum integral of the wake ($= U_0^2 W_0 b$)
M_1	Momentum integral of the wake at station D
P	Mean static pressure at any point
P_B, P_C	Average static pressure at stations B and C
P_w	Wall static pressure at any point

P_{wA}	Wall static pressure at reference station A
q_B	Dynamic pressure at station B
U	Streamwise component of mean velocity
$\bar{U}$	Mean velocity at any station
U_c	Mean velocity along the axis of the wake in the streamwise direction
U_{max}	Maximum mean velocity at any station in streamwise direction
U_o	Local free-stream velocity
$U_{\infty A}$	Mean free-stream velocity at reference station A
u_τ	Shear velocity ($= \tau_w / \rho)^{1/2}$
W	Defect velocity in the wake ($= U_o - U$)
W_o	Maximum defect velocity in the wake ($= U_o - U_c$)
X	Distance measured from the trailing edge of the airfoil along the axis of the diffuser
x	Distance measured along the wall
y	Distance from the wall measured normal to the axis of the diffuser
y^+	$= yu_\tau / \nu$
α	Incidence angle of the airfoil
β_w	Relative wake depth ($= W_o / U_o$)
δ	Boundary layer thickness
δ^*	Displacement thickness
η	Normalised distance for the wake ($= y_A / b_A$, y_B / b_B)
ρ	Mass density of the fluid
ν	Kinematic viscosity of the fluid
τ_w	Wall shear stress

References

1. WAITMAN, B.A., RENEAU, L.R. AND KLINE, S.J. — Effects of inlet conditions on performance of two-dimensional subsonic diffusers, *J. Basic Engng., Trans. ASME*, 1961, **83**, 349-360.
2. WOLF, S. AND JOHNSTON, J.P. — Effects of nonuniform inlet velocity profiles on flow regimes and performance in two-dimensional diffusers, *J. Basic Engng., Trans. ASME*, 1969, **91**, 462-474.
3. RENEAU, L.R. JOHNSTON, J.P. AND KLINE, S.J. — Performance and design of straight, two-dimensional diffusers, *J. Basic Engng. Trans. ASME*, 1967, **89**, 141-150.
4. PIERCE, F.J. AND ZIMMERMAN, B.B. — Wall shear stress inference from two and three-dimensional turbulent boundar layer velocity profiles, *J. Fluids Engng., Trans. ASME*, 1973, **95**, 61-67.
5. IRWIN, H.P.A.H. — Measurements in a self-preserving plane wall jet in a positive pressure gradient, *Fluid Mech.* 1973, **61**, 33-63.
6. SCHUBAUER, G.B. AND SPANGENBERG, W.G. — Forced mixing in boundary layers, *J. Fluid Mech.*, 1960, **8**, 10-32.
7. SOVRAN, G. AND KLOMP, E.D. — Experimentally determined optimum geometries for rectilinear diffusers w rectangular, conical or annular cross-section. In *Fluid mechanics of internal fl* edited by G. Sovran, Elsevier Publishing Co., 1967, 270-319.
8. CHITHAMBARAN, V.K. — Some studies of the structures of incompressible turbulent flow in a two-dimensio diffuser with inlet velocity distortion, Ph.D. thesis, Indian Institute of Technolo Madras, 1978.
9. CLAUSER, F.H. — Turbulent boundary layers in adverse pressure gradients, *J. Aero. Sci.*, 1954, **21**, 91-1
10. LUDWIEG, H. AND TILLMANN, W. — Investigations of the wall-shearing stress in turbulent boundary layers, NACA T 1285, 1950.

11. SPANGENBERG, W.G. ROWLAND, W.R. AND MEASE, N.E. Measurements in a turbulent boundary layer maintained in a nearly separating condition. In *Fluid mechanics of internal flow* edited by G. Sovran, Elsevier Publishing Co., 1967, pp. 110-151.

12. NASH, J.F. Turbulent boundary layer behaviour and the auxiliary equation, NPL Aero. Rep. ER. 1137, 1965.

13. COLES, D. The law of the wake in the turbulent boundary layer, *J. Fluid Mech.* 1956, **1**, 191-226.

14. URAM, E.M. Discussion, separation prediction for conical diffusers, *J. Basic Engng., Trans. ASME.*, 1960, **82**, 207-208.

15. SPENCE, D.A. Growth of the turbulent wakes close behind an aerofoil at incidence, ARC CP 125, 1953.

16. RAJ, R. AND LAKSHMINARAYANA, B. Characteristics of the wake behind a cascade of airfoils, *J. Fluid Mech.*, 1973, **61**, 707-730.